

CHAPTER 2

CuO nanostructures

2.1 Literature review of preparation of CuO nanostructures

CuO nanostructures can be synthesized by various growth techniques such as thermal evaporation, thermal decomposition or oxidation. Oxidation is one of the more practical and simple ways of synthesis and most commonly used for the synthesis of CuO nanostructures.

Huang and co-workers⁽⁵⁾ synthesized CuO nanowires by thermal evaporation using copper foil in an O₂ ambient at temperatures from 300 to 900°C. SEM, TEM, high-resolution transmission electron microscopy (HRTEM) and X-ray diffraction (XRD) were performed. The growth of the nanowires seemed to follow the vapor–solid (VS) mechanism. When the evaporation temperature was as high as 800°C, only a small amount of CuO fibers were formed. At evaporation temperatures from 400 to 750°C, large amount of CuO nanowires with diameters between 70–100 nm can be prepared. With increase of the evaporation time, the length of the nanowires increased, but the growth rate decreased. XRD studies revealed the possibility of two-steps of nanowire formation; HRTEM image shows the bicrystal structure of the nanowire; SEM studies indicate the relationship between the morphology of the prepared nanowires and the growth conditions. The large-scale CuO nanowires reported here can be used as semiconductors, gas sensors and catalysts. The prepared CuO nanowires are shown in figure 2.1.

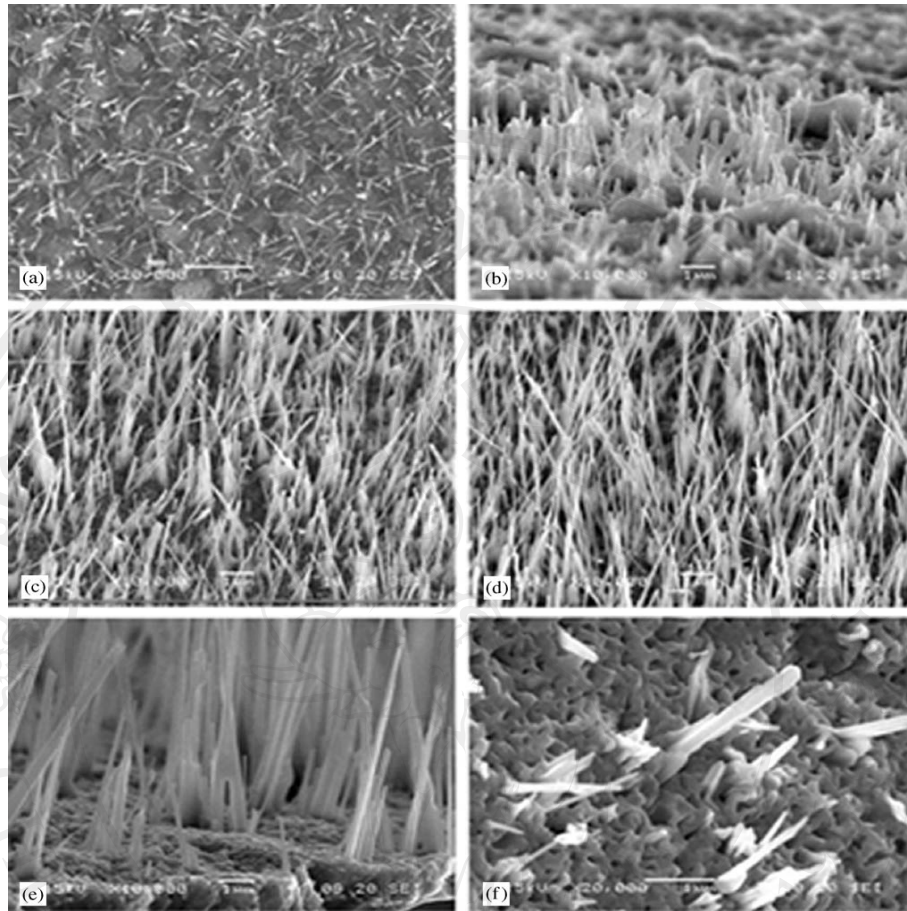


Figure 2.1 SEM images of CuO nanowires prepared by thermal evaporation at various temperatures: (a) 300, (b) 400, (c) 500, (d) 600, (e) 750 and (f) 800°C⁽⁵⁾.

Kaur and co-worker⁽⁷⁾ prepared CuO nanowires by thermal oxidation using copper foils in an oxygen atmosphere. Morphology and microstructure of the nanowires were studied as a function of temperature (between 500 to 800°C) and annealing time using scanning electron microscopy (SEM), energy dispersive X-ray analysis, X-ray diffractogram, X-ray photo electron spectroscopy, transmission electron microscopy (TEM) and selected area electron diffraction (SAED). Nanowires in hills are thinner (50-100 nm) and longer (7-15 mm) and those in valleys are thicker (100-200 nm) and shorter (14 mm). Nanowires were found to grow preferentially

along [010] direction and branches along [210] direction. The band gap of CuO nanowires was found to be larger than that of bulk material. The prepared CuO nanowires are shown in figure 2.2.

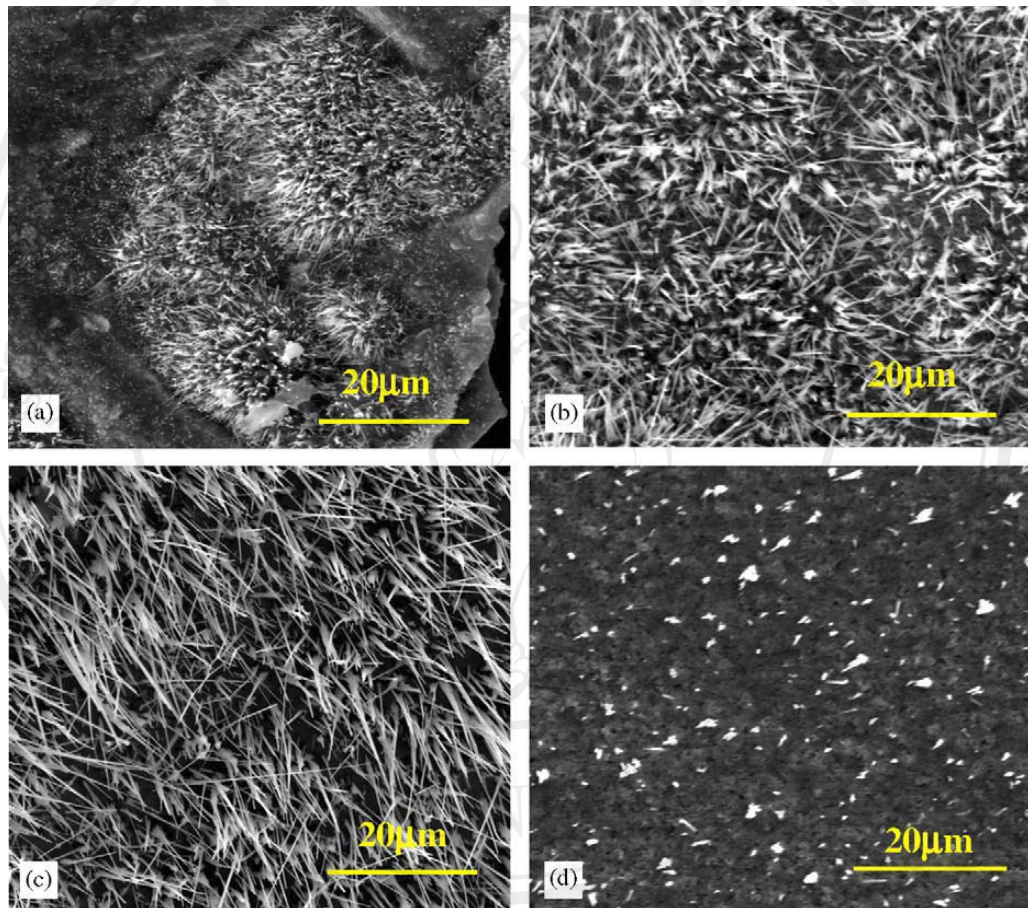


Figure 2.2 SEM micrographs of CuO nanowires prepared by annealing copper strips for 4 hr under oxygen atmosphere at different temperatures: (a) 500, (b) 600, (c) 700 and (d) 800°C⁽⁷⁾.

Wang and co-workers⁽⁴⁾ synthesized CuO nanoparticles by microwave irradiation, using copper (II) acetate and sodium hydroxide as the starting materials and ethanol as the solvent. The CuO nanoparticles were characterized by using

techniques such as XRD, TEM, SAED, X-ray photoelectron spectroscopy and UV–Visible absorption spectroscopy. The as-prepared CuO nanoparticles have regular shape, narrow size distribution and high purity. The band gap is estimated to be 2.43 eV according to the results of the optical measurements of the CuO nanoparticles. It is a simple and efficient method to produce CuO nanoparticles with regular shape, small size, narrow size distribution and high purity. They can foresee the upscaling of the process to form large quantities of CuO nanoparticles, which have wide applications in various fields such as photonics, catalysis and biosensors. The prepared CuO nanoparticles are shown in figure 2.3.

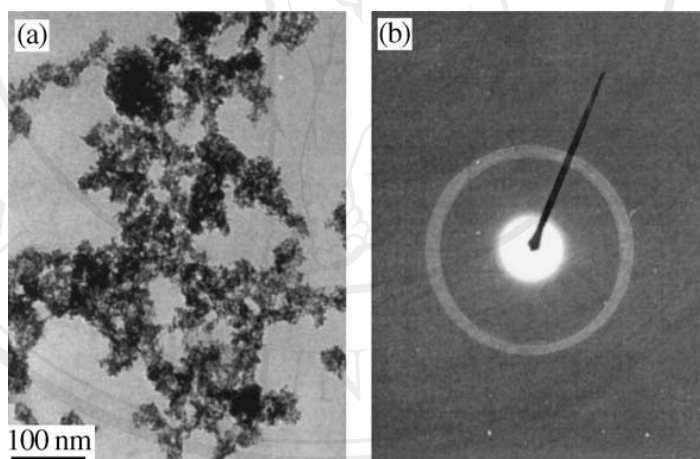


Figure 2.3 (a) TEM and (b) electron diffraction pattern of the as-prepared CuO nanoparticles⁽⁴⁾.

Wang and co-workers⁽¹⁵⁾ synthesized CuO nanowhiskers by a novel one-step, solid-state reaction in the presence of nonionic surfactant, PEG 400. The CuO nanowhiskers have average size of approximately 8 nm in diameter and of length scales larger than 100 nm. The rod shape nature of the CuO nanowhiskers have been

analyzed by TEM, XRD, HRTEM and XPS. The easy and unique solid state synthesis in the presence of nonionic surfactant, PEG 400, may be extended to the synthesis of other nanoparticles, nanorods and semiconductors, e.g. ZnS, CuS, PbS, NiS, FeS and CdSe. The prepared CuO nanowhiskers are shown in figure 2.4.

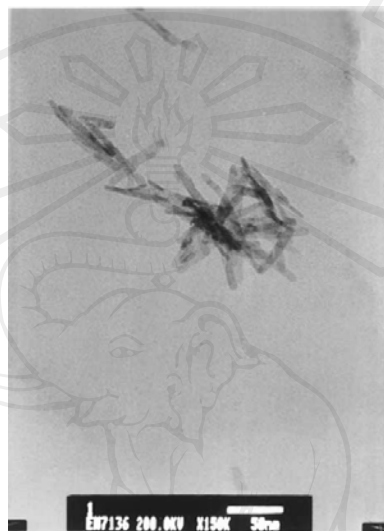


Figure 2.4 TEM image of the CuO nanowhiskers⁽¹⁵⁾.

Xu and co-workers⁽⁶⁾ synthesized CuO nanorods by thermal decomposition of CuC_2O_4 obtained via chemical reaction between $\text{Cu}(\text{CH}_3\text{COO})_2\text{H}_2\text{O}$ and $\text{H}_2\text{C}_2\text{O}_4\cdot 2\text{H}_2\text{O}$ in the presence of surfactant nonyl phenyl ether (9)/(5)(NP-9/5) and NaCl flux. The results showed that the nanorods were composed of CuO with diameter of 30–100 nm, and length ranging from 1 to 3 μm . XRD, TEM, XPS, SAED and HRTEM were used to characterize the structure features and the chemical composition of the nanorods. The prepared CuO nanorods are shown in figure 2.5.

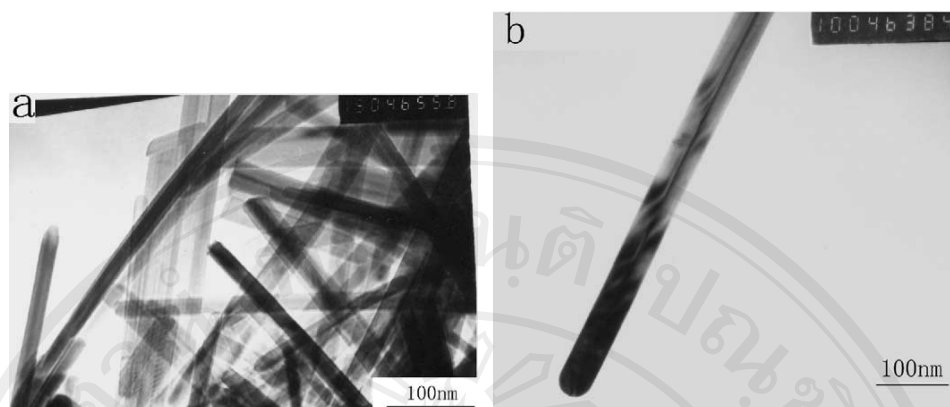


Figure 2.5 TEM images of the as-prepared CuO nanorods. (a) Morphologies of the as-prepared CuO nanorods. (b) Morphology of the as-prepared single CuO nanorod⁽⁶⁾.

Xu and co-worker⁽¹⁶⁾ prepared CuO nanoparticles by a one-step solid state reaction under ambient conditions. $\text{CuCl}_2 \cdot 2\text{H}_2\text{O}$ and NaOH in a molar ratio of 2:5 were mixed and ground, and a short induction followed. The color of the mixtures gradually changed from bluish to black, indicating the formation of CuO. After grinding for 30 min, the black product was washed with an ultrasonic wave, then three times in distilled water and twice in alcohol, and then dried in air. The purity of the product was analyzed by inductively coupled plasma-atomic emission spectroscopy (ICP-AES), and no more than 100 ppm of any impurity was detected. The CuO particles with an average size of 12 nm were pressed into pellets under high pressure. They were studied by X-ray photoelectron spectroscopy (XPS), XRD, TEM, and Raman spectroscopy. The CuO grains in pellets grow with time at room temperature. The gradual increase in the grain size with time is clearly respected in their Raman spectra and the XRD results. The prepared CuO nanoparticles were shown in figure 2.6.

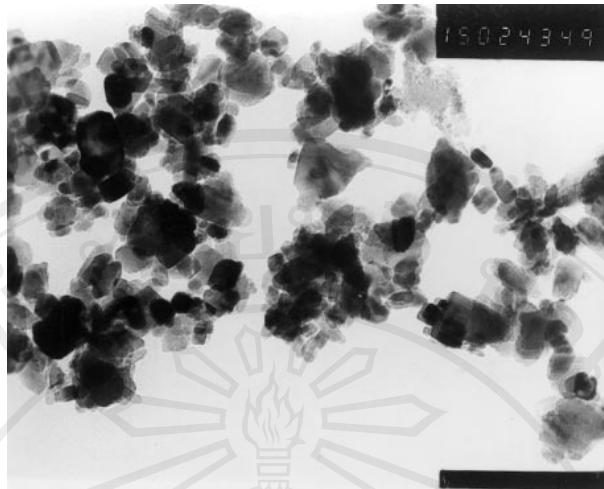


Figure 2.6 TEM micrograph image of the CuO particles ($\times 150,000$)⁽¹⁶⁾.

Xu and co-workers⁽¹⁷⁾ prepared CuO nanowires using copper foils by oxidization in wet air at temperatures from 300 and 800°C. Within the temperature range of 400-700°C, the nanowires formed have two different morphologies, curved and straight, with diameters between 50 and 400 nm and lengths between 1 and 15 μm . The growth behavior can be understood in terms of kinetics involving short-circuit diffusion, the strength of the nanowires, and the thickness ratio of the oxide scale and the metal. Increasing the oxidation temperature may produce a reduction in the density, but an increase in the diameter and strength, of the nanowires, causing them to adopt a straight morphology. The kinetics of the formation of CuO nanowires is governed by the short-circuit diffusion of atoms or ions during the reaction. The deformation of thin oxide scale under thermal stresses may also contribute to the formation of curved nanowires. Other factors may also contribute to facilitate the growth of CuO nanowires, such as thin specimens, which favor the formation of the CuO phase. The prepared CuO nanowires are shown in figure 2.7.

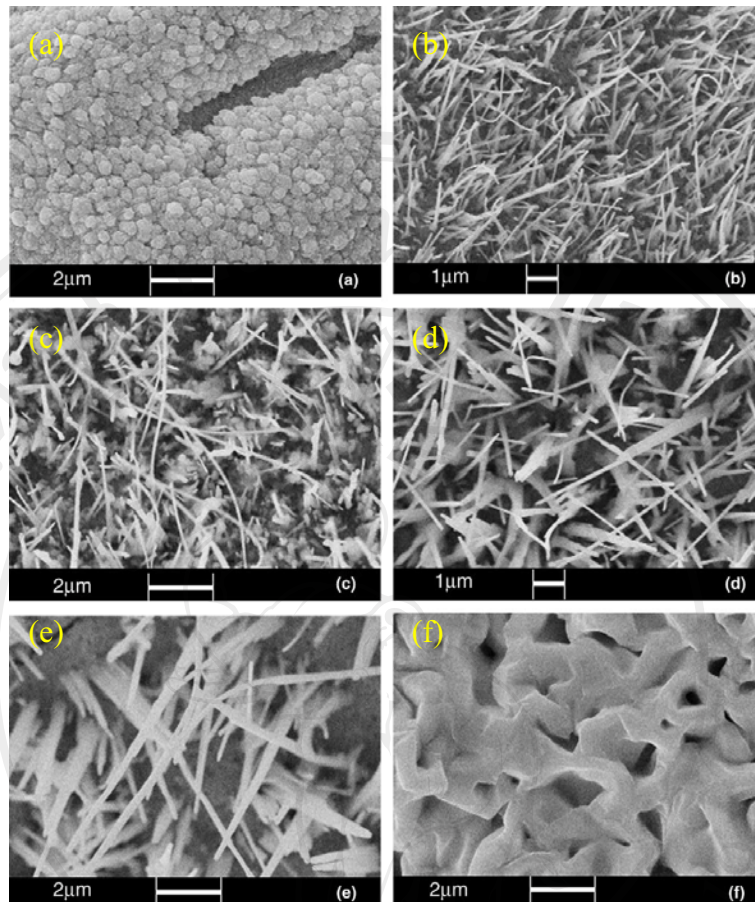


Figure 2.7 The morphologies of the oxide scales formed on Cu foils at: (a) 300°C, showing round oxide grains, (b) 400, (c) 500, (d) 600, (e) 700°C, showing nanowires with different density, size and shape and (f) 800°C, showing oxide crystals⁽¹⁷⁾.

2.2 Preparation of CuO nanostructure

Different types of CuO nanostructures such as nanowires and thin films were prepared by different method for use as a p-type semiconductor for application in ethanol sensor and DSSC.

2.2.1 CuO nanowires by oxidation of copper plate

CuO nanowires were prepared by thermal oxidation reaction method using commercial copper plate (commercial grade) with dimension of 2×4 cm. The copper

plate was cleaned by acetone then it was heated to temperatures of 300, 400, 500, 600, 700 and 800°C in normal atmosphere for 6 hr to achieve oxidation reaction. After oxidation via heating, the copper plate was immediately taken from the furnace and cooled down in air. The colour of the copper plate changed to black after the oxidation reaction. It has been reported that the colour of CuO, Cu₂O and Cu are black, red and copper, respectively. The obtained CuO nanowires were characterized by Field Emission Scanning Electron Microscope (FE-SEM, JEOL JSM-6335F), Energy Dispersive Spectroscopy (EDS) and Transmission Electron Microscope (TEM, JEOL JEM-2010 operating at 200 kV) for morphology, chemical composition and crystal structure, respectively. The result was discussed in section 2.3.

2.2.2 CuO nanowires by oxidation of copper powder

CuO nanowires were prepared by thermal oxidation reaction method using high purity (99.9%) copper powder. The powder was screened onto conducting glass by doctor blade method with PEG (polyethylene glycol) binder with sized of screen 0.5×2 cm and then heated at 400°C in normal atmosphere for 7 hr; 1 hr for remove PEG and 6 hr for oxidation reaction. After oxidation reaction via heating, the conducting glass was cooled down in the furnace. The colour of the copper powder changed to black after oxidation reaction. The obtained CuO nanowires were characterized by FE-SEM and EDS for morphology and chemical composition, respectively. The result was discussed in section 2.3.

2.2.3 CuO thin films by oxidation of copper thin films

CuO thin films were prepared by oxidation reaction of copper thin films. Copper thin films were prepared by thermal evaporation method using high purity (99.9%) copper powder. The powder was placed in an electric boat at pressure of 0.4

mTorr in a vacuum tube. The films were evaporated onto an alumina substrate. The substrate used in this process had dimensions of 20×30 mm and was first cleaned by alcohol in an ultrasonic bath for 2 min and dried at room temperature. The distance between the electric boat and the substrate was 7 cm and the temperature of the substrate was kept at room temperature. After thermal evaporation, the copper thin films were loaded into the central position of a tube furnace and heated to 400, 500, 600, 700, 800 and 900°C at normal atmosphere for oxidation reaction. After oxidation reaction of 12, 24 and 48 hr, the colour of the copper thin films changed to black. The obtained black products were investigated by FE-SEM for morphology, EDS for chemical composition, and XRD for crystal structure. The result was discussed in section 2.3.

2.3 Properties of CuO nanostructures

2.3.1 CuO nanowires by oxidation of copper plate

CuO nanowires were prepared by oxidation reaction of copper plate with different heating temperature such as 300, 400, 500, 600 and 700°C for 6 hr in atmosphere. The top view and cross section of the black CuO product were investigated by 1) FE-SEM to analyze morphology, 2) EDS to analyze chemical composition, 3) TEM to analyze crystal structure and to find the growth direction of the crystal and 4) Raman spectroscopy for Raman peak.

2.3.1.1 FE-SEM of CuO nanowires by oxidation of copper plate

The product of annealing copper plate (black colour) was analyzed by FE-SEM. Figure 2.8 shows FE-SEM top view images of the black products heated at (a) 300, (b) 400, (c) 500, (d) 600, (e) 700 and (f) 800°C, in normal atmosphere

respectively. Figure 2.8(a) shows the round oxide grains with diameters of about 300 nm at 300°C, with low density of nanowires on the surface of the specimen. Nanowires form at temperatures of 400–700°C. Figure 2.8(b) shows the morphologies of nanowire scales formed at 400°C. This figure shows a high density of uniformly curved nanowires, with diameters in the range of 50 to 300 nm and lengths of 1–3 μm . The nanowires formed at 500°C also have a high density and the size of the nanowires is uniform, with lengths ranging from 1 to 15 μm and diameters from 100 to 300 nm as shown in figure 2.8(c). The nanowires formed at 600°C still have a high density, lengths of 2–15 μm and diameter of 70–200 nm and the size of the nanowires are uniform, as shown in Figure 2.8(d). Comparing the nanowires formed at 500°C, the nanowires formed at 600°C are more uniform and straight. Nanowires formed at 700°C as shown in Figure 2.8(e) have a low density and are straight with diameters in the range of 120–1000 nm and lengths of 2–15 μm . Large oxide grains were formed during oxidation reaction at 800°C as shown in Figure 2.8(f), which is caused by crystal growth.

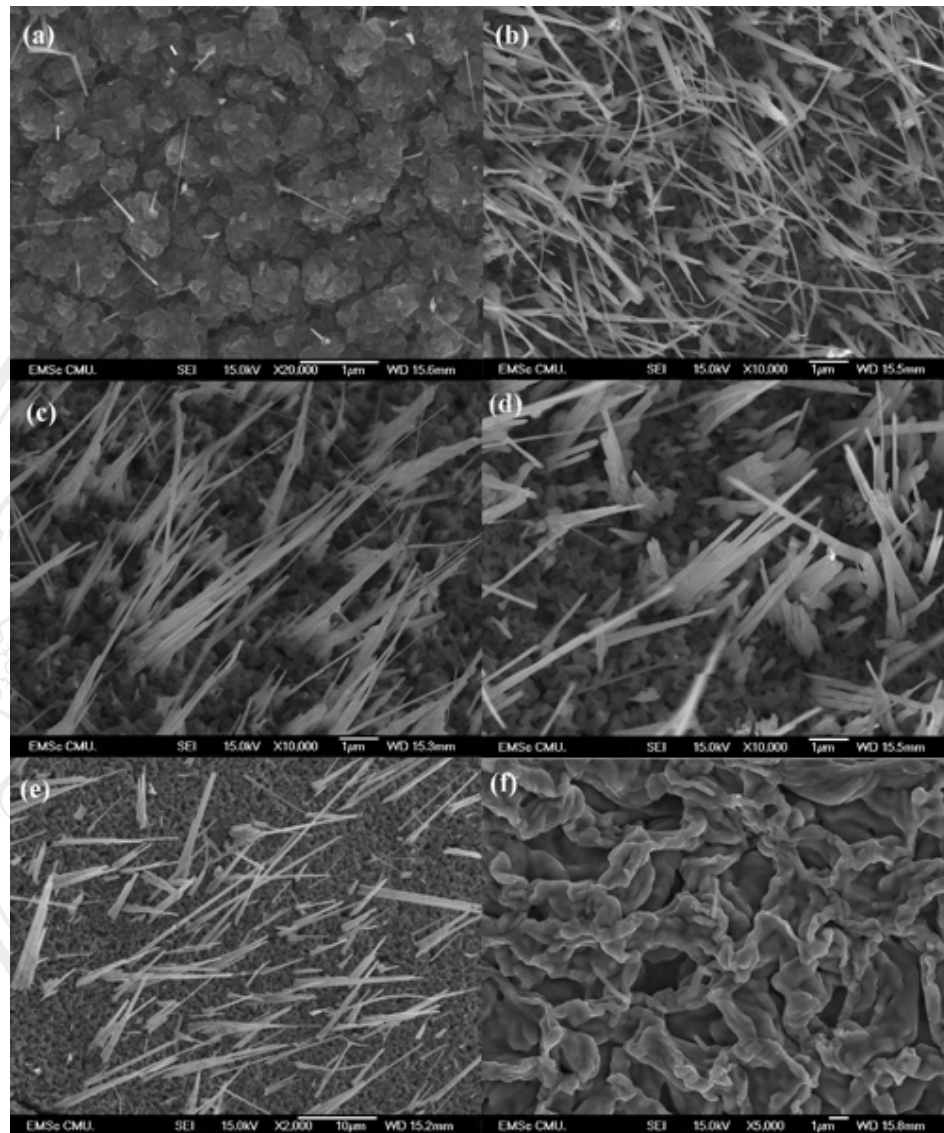


Figure 2.8 FE-SEM top view images of thermal oxidation reaction of copper plate at

(a) 300, (b) 400, (c) 500, (d) 600, (e) 700 and (f) 800°C in normal atmosphere.

Figure 2.9 shows a FE-SEM cross-section image of a copper plate heated at 600°C at x 1,000 magnification. From the cross-section image there are three zones that can be observed. The first layer in the bottom of figure is a thick layer with red colour which is Cu_2O structure phase. The middle layer is of black colour with thickness of 4.2 μm which is CuO structure phase. The top layer is the zone of CuO

nanowires with black colour. The discussion of the EDS result of Cu_2O , CuO and CuO nanowires will be discussed in the following section.

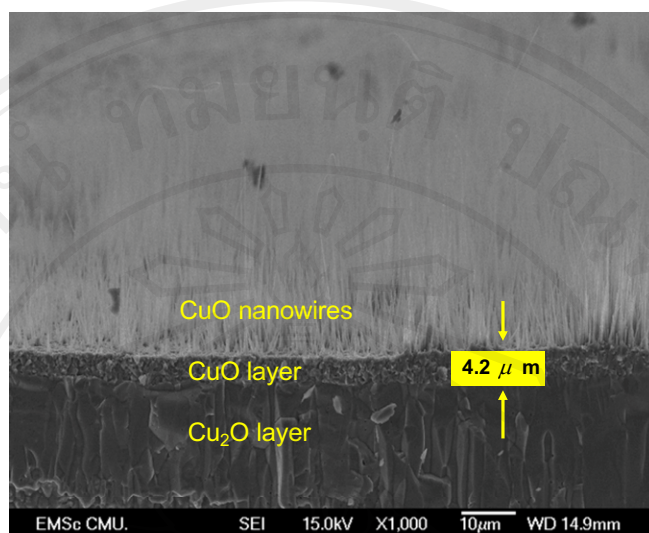


Figure 2.9 FE-SEM cross-section image of thermal oxidation reaction of copper plate at 600°C .

2.3.1.2 EDS result of CuO nanowires by oxidation of copper plate

EDS spectrum measurements were performed on each zone of the copper plate. The top zone, the middle and the first zone of copper plate were selected to measured EDS spectra as shown in figure 2.11, 2.13 and 2.15, respectively. The EDS spectrum on the middle layer is similar to the EDS spectrum of nanowires as shown in figure 2.11 and 2.13. Atomic percent of copper and oxygen are reported in Tables 2.1, 2.2 and 2.3 for CuO nanowires, CuO layer and Cu_2O layer, respectively. The atomic ratio of copper and oxygen obtained from the EDS spectrum is 42:58 for the top layer as shown in Table 2.1, 52:48 for the middle layer as shown in table 2.2 and 31:69 for the bottom layer as shown in Table 2.3. It means that the atomic ratio of copper and oxygen are approx 1:1, 1:1 and 1:2 which can be approximately assigned to CuO and

Cu₂O layer. Therefore, the thick Cu₂O layer should firstly be formed on the copper plate, followed by the formation of the CuO layer and then CuO nanowires finally formed on the CuO layer. The process of oxidation reaction of copper plate is shown in figure 2.16. However, the growth mechanism of CuO nanowires remains to be investigated.

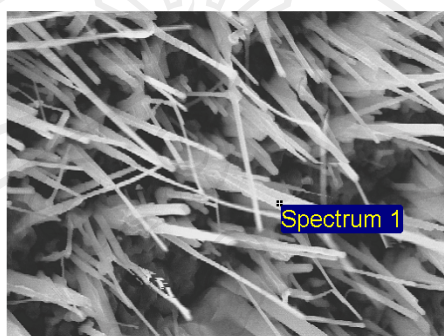


Figure 2.10 EDS spectrum selection of CuO nanowires.

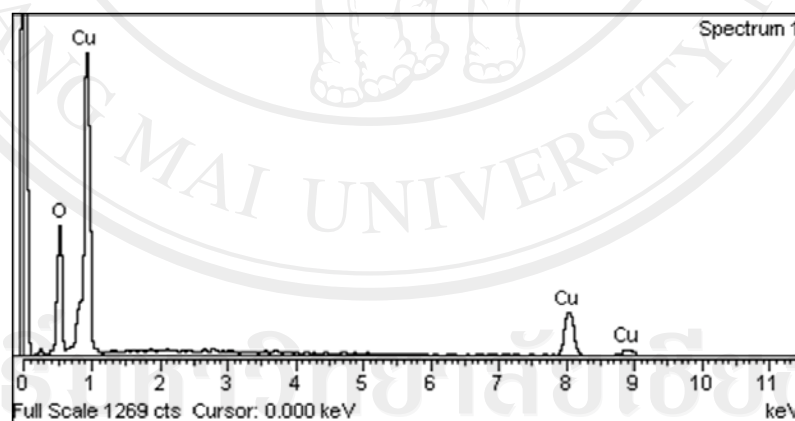


Figure 2.11 EDS spectrum of CuO nanowires.

Table 2.1 Element content of CuO nanowires

Element	Weight%	Atomic%
O	25.49	57.60
Cu	74.51	42.40
Total	100.00	100.00

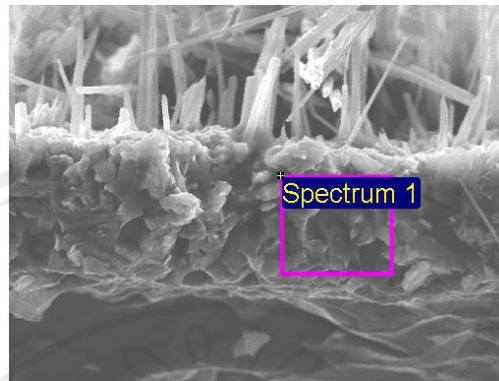


Figure 2.12 EDS spectrum selection of CuO layer.

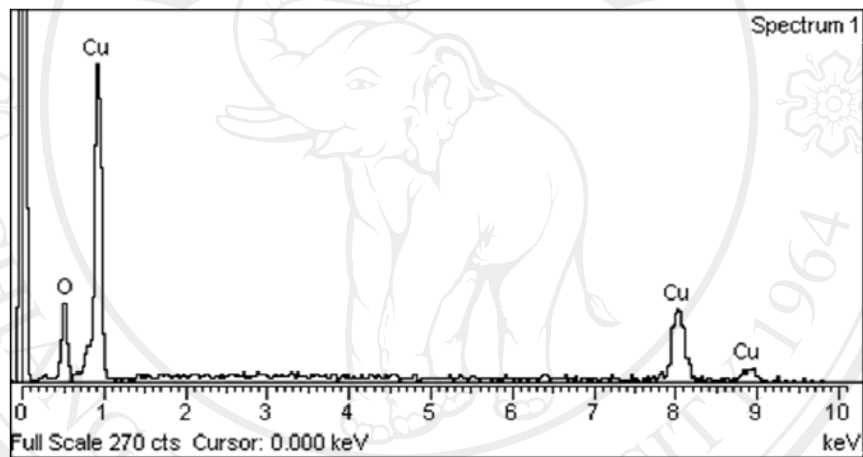


Figure 2.13 EDS spectrum of CuO layer.

Table 2.2 Element content of CuO layer

Element	Weight%	Atomic%
O	19.12	48.42
Cu	80.88	51.58
Total	100.00	100.00

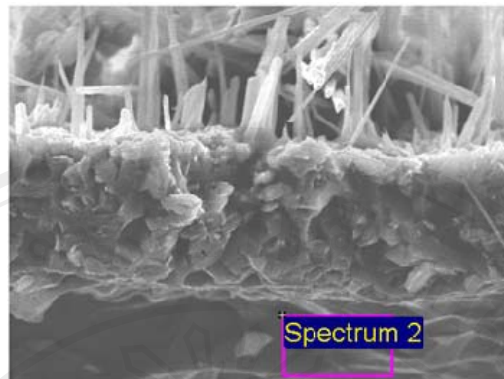


Figure 2.14 EDS spectrum selection of Cu_2O layer.

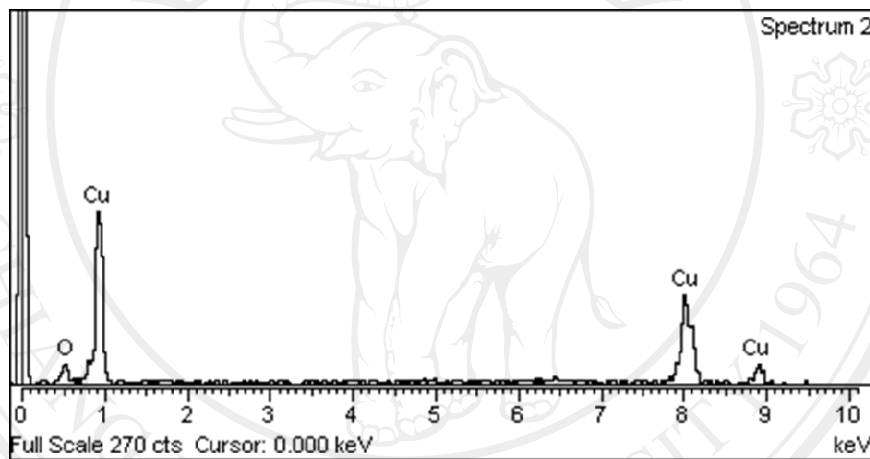


Figure 2.15 EDS spectrum of Cu_2O layer.

Table 2.3 Element content of Cu_2O layer

Element	Weight%	Atomic%
O	10.01	30.64
Cu	89.99	69.36
Total	100.00	100.00

When copper is oxidized in air, the major product is Cu_2O , and CuO is formed slowly only through a second step of oxidation. In this case, Cu_2O served as a precursor to CuO . The reactions involved in the entire synthesis are summarized as follows, with the second one functioning as the rate-determining step for the

formation of CuO vapor follow in Equations (2.1) and (2.2)⁽¹⁸⁾. The oxidation reaction of copper is shown in figure 2.16.

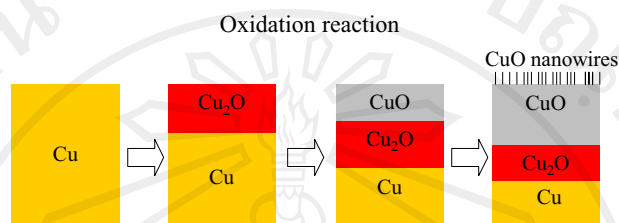


Figure 2.16 Oxidation reaction process of copper plate.

The slow rate for the formation of CuO ensures a relatively low vapor pressure for this material in the reaction chamber. Thus, this result in a continuous growth mode and uniform diameter for the CuO nanowires. It was found that the amount of CuO nanowires depend on the oxidation reaction temperature and the diameter of CuO nanowires were increase with the increasing oxidation reaction temperature as shown in Table 2.4.

Table 2.4 Show the amount of CuO nanowires per $10 \mu\text{m}^2$ and diameter of the nanowires.

Oxidation reaction temperature (°C)	Amount of nanowires per $10 \mu\text{m}^2$	Diameter of nanowires (nm)
300	40-50	Less than 100
400	3000	20-150
500	2000	100-300
600	2000	100-400
700	100-20	200-1000

2.3.1.3 TEM result of CuO nanowires by oxidation of copper plate

The results from TEM investigation of CuO nanowires from oxidation at 600°C are shown in figure 2.17 and 2.18. Figure 2.17 shows the rotation bright field image of CuO (a) projection at 0° and (b) projection at 76°, respectively this result confirms wire-like structure of A.

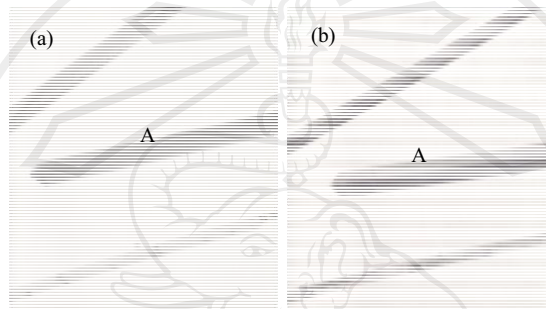


Figure 2.17 TEM Bright field image of CuO nanowires (a) projection at 0° (b) projection at 76°.

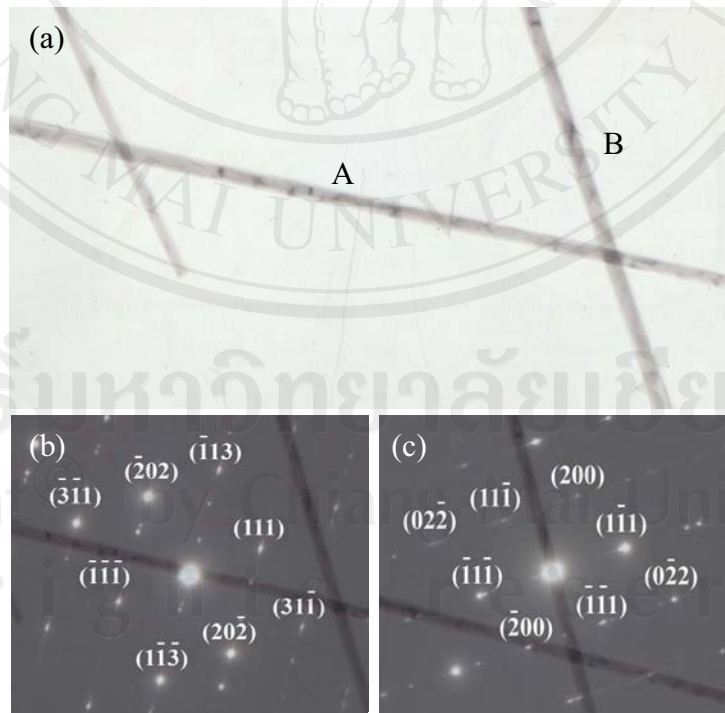


Figure 2.18 (a) bright field image of CuO nanowires, (b) SADP of CuO nanowire at line A and (c) SADP of CuO nanowire at line B.

Figure 2.18 (a) shows TEM bright field image of CuO nanowires were heated at 600°C with the associated SADP in Figure 2.18 (b) and (c). The three lines of wire-like structure can be observed from the TEM image. The SADP of the wires marked A and B of CuO nanowire show a spot pattern, indicating single-crystalline property of the nanowire which corresponds to the monoclinic structure of CuO with lattice constants, $a = 4.7 \text{ \AA}$, $b = 3.4 \text{ \AA}$ and $c = 5.1 \text{ \AA}$. The spots can be indexed as shown in Figure 2.18 (b) and (c). The SADP also confirms the EDS result that the nanowire is CuO.

2.3.1.4 Raman spectra result of CuO nanowires by oxidation of copper plate

CuO nanostructure has monoclinic crystal structure with C_{2h}^6 space group symmetries. There is 5 atomic unit cell having two molecules per primitive cell within (2.3).

$$\Gamma = 4A_u + 5B_u + A_g + 2B_g \quad (2.3)$$

Then, there are twelve zone-center optical-phonon modes ($3n-3$), three acoustic modes ($A_u + 2B_u$), six infrared active modes ($3A_u + 3B_u$) and three Raman active modes ($A_g + 2B_g$). In this work, all the Raman spectra were recorded under the backscattering geometry of Raman. Typical Raman spectra of the CuO nanostructure as a function of wave number are shown in figure 2.19.

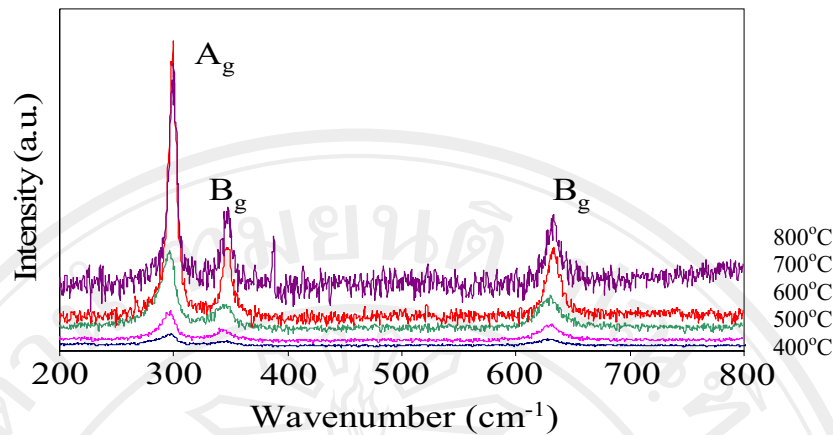


Figure 2.19 Raman shift of CuO nanowires with difference oxidation temperature.

Three peaks of CuO at 296.4, 345.9 and 633.3 cm^{-1} , correspond to the A_g (296 cm^{-1}), B_g (346 cm^{-1}), and B_g (636 cm^{-1}) modes of bulk CuO crystals, respectively. That is broadening of Raman spectra increase with decrease in grain size.

2.3.2 CuO nanowires by oxidation reaction of copper powder

2.3.2.1 FE-SEM of CuO nanowires by oxidation of copper powder

After oxidation reaction of copper powder, the colour of the copper powder turned into black. The annealed copper powder was investigated by FE-SEM for morphology. Figure 2.20 shows FE-SEM images of the copper powder heated at 400°C. The morphology exhibits CuO nanowires with dimensions in the range 50-200 nm in diameter and 5 μm in length. It shows that nanowires were established from the surface of copper powder. With the same conditions of heating temperature as the copper plate it can assume that the nanowires on the top of the copper powder are CuO nanowires.

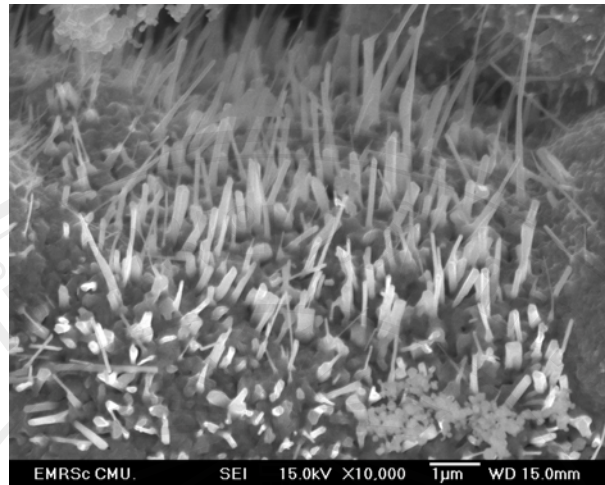


Figure 2.20 FE-SEM top view images of CuO nanowires on copper powder.

2.3.3 Growth mechanism of metal-oxide nanowire⁽¹⁹⁾

The growth mechanism of metal-oxide nanowire is proposed as in the following four steps: 1. oxygen adsorption, 2. surface oxidization to form nuclei, 3. nuclei arrangement and 4. nanowire formation as shown in figure 2.21.

Step 1. oxygen adsorption: Typically, oxygen molecules in air are adsorbed on the metal surface with diffusion process. There are many reports to describe the mechanism of O_2 interaction with the transition metal surface⁽²⁰⁾.

Step 2. surface oxidization to form nuclei: the metal-oxide nucleation was formed by diffusion of metal ions and/or oxygen ions in the oxide layer, and the reactions of metal ions with oxygen ions to form metal-oxide. To form nuclei of metal-oxide in the oxide layer (as in figure 2.22), metal-oxide nucleus is formed by agglomeration between metal ion and oxygen ion due to the minimization of surface energy. This phenomenon is similar to the coalescence behavior of two droplet of water when they are connected and then forming bigger one droplet instead of staying separately. In order to explain the growth mechanism, Gibb free energy change per

nucleus (not per mole) of metal-oxide with radius r and volume V is introduced and defined as

$$\Delta G_N = V\Delta G^0 + A_f\gamma_f \quad (2.4)$$

where A_f and γ_f is surface area and surface energy, respectively. For a given ΔG^0 which is usually negative, the magnitude of ΔG_N depends on only two terms: a volume energy and surface energy. Volume energy is proportional to $-r^3$, but surface energy is proportional to r^2 . Thus, ΔG_N as a function of r exhibits maximum value at some critical radius, r^* , as seen in figure 2.21 (c).

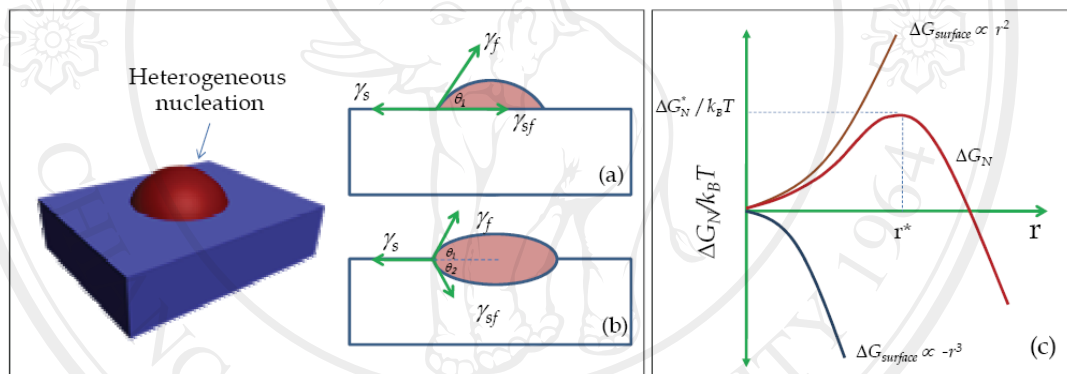


Figure 2.21 Model of the metal-oxide nucleation for (a) non-reactive and, (b) reactive nucleation and (c) plot of ΔG_N as a function of radius⁽¹⁹⁾.

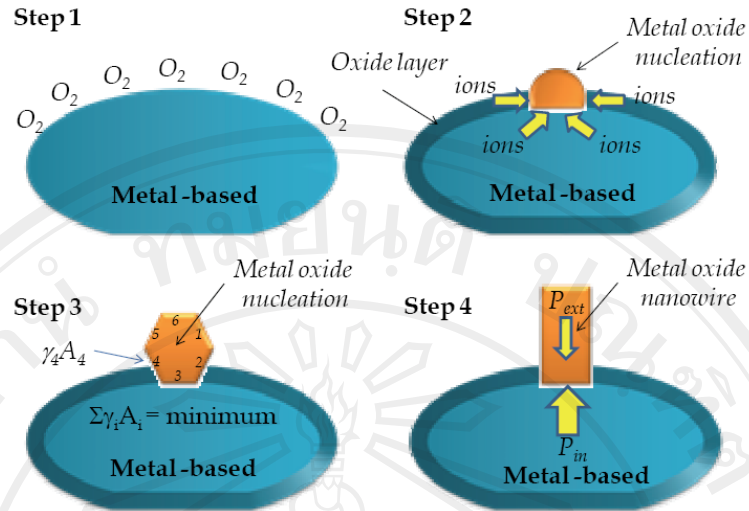


Figure 2.22 Four steps of metal-oxide nanowire growth mechanism, Step 1 - oxygen adsorption, Step 2 - surface oxidation to form nuclei, Step 3 - nuclei arrangement and finally, Step 4 - nanowire formation ⁽¹⁹⁾.

Step 3. nuclei arrangement: the metal-oxide nuclei arrangement was designed based on the nuclei probability in term of the minimization of surface energy. As discuss above, a nucleation will form when it can overcome the maximum energy barrier, ΔG_N^* . Thus, it can write the probability of nucleation, P_N , and given

$$P_N = \frac{N}{N_0} = \exp(-\Delta G_N^*) / k_B T \quad (2.5)$$

where N is the surface concentration of nuclei and N_0 is the possible surface concentration of nuclei on metal surface, k_B is Boltzmann constant and T is temperature. It can be seen that the magnitude of P_N depends on three parameters; temperature, surface energy, and ΔG^0 . For temperature effect, it can be seen that the probability increases when the temperature increases at constant surface energy and ΔG^0 . Therefore, the number of nanowires can be explained in term of nucleation frequency.

Step 4. nanowire formation: nanowire was grown by the driving force from the difference of the surface pressure between metal-oxide nucleation and substrate (or metal based). First, let consider the pressure inside the particles, which have radius r and surface energy γ as given by Laplace equation as

$$P_i = P_g + \frac{2\gamma_i}{r_i} \quad (2.6)$$

where P_g is the external pressure in the surrounding, subscript i referred to the solid or liquid phase. We will now consider a case where metal-oxide nucleation as a solid phase with radius r_f adsorbs on metal-based substrate with radius r_l . At interface between metal-oxide nucleation and substrate, which has surface energy γ_{sf} , the different pressure at interface is

$$P_s - P_l = \frac{2\gamma_s}{r_s} - \frac{2\gamma_l}{r_l} \quad (2.7)$$

In our case, we assumed that the substrate or metal-based has a large radius r_l , so the second term in Eq.2.7 should be neglected. Therefore, we can write the differential form of Eq. 2.7 as

$$d(P_s - P_l) = d\left(\frac{2\gamma_{sf}}{r_s}\right) \quad (2.8)$$

Integrating from a flat interface ($r = \infty$), we obtained

It can be seen that the different pressure is inversely proportional to nucleation radius at certain surface.

First, the Cu was easily oxidized to form Cu_2O layer due to the Cu_2O has lower oxidization Gibb free energy than CuO as showed in figure 2.9. So, we will consider the Cu_2O as the substrate for creation CuO nucleation. Similar to ZnO case,

the CuO nuclei were formed and arranged based on the minimization of total surface energy. After that, the driving force for CuO nanowires was produced by the small size of CuO nucleation. The growth mechanism is confirmed by the cross-section FE-SEM image of CuO nanowire on Cu substrate as shown in figure 2.9. It can be seen that the thick Cu₂O layer is firstly formed on copper plate, followed by the formation of CuO layer and then CuO nanowires was finally formed on CuO layer.

2.3.4 CuO thin films by oxidation of thermal evaporated copper thin films

2.3.4.1 FE-SEM result of CuO thin films by thermal evaporated copper thin films

CuO thin films were prepared by oxidation reaction of thermal evaporation as shown in figure 2.23. This figure shows FE-SEM top view image of the copper thin films before and after oxidation reaction at 300°C, 400°C, 500°C (in atmosphere) for, 600°C, 700°C, 800°C for 48 hr and 900°C for 12 hr. The nanostructures with diameter of 100-600 nm were observed. It was shown that the size of nanostructure depend on oxidation reaction time and oxidation reaction temperature. The thickness of CuO thin films is around 1 μm that confirms in figure 2.24 by FE-SEM cross-section image.

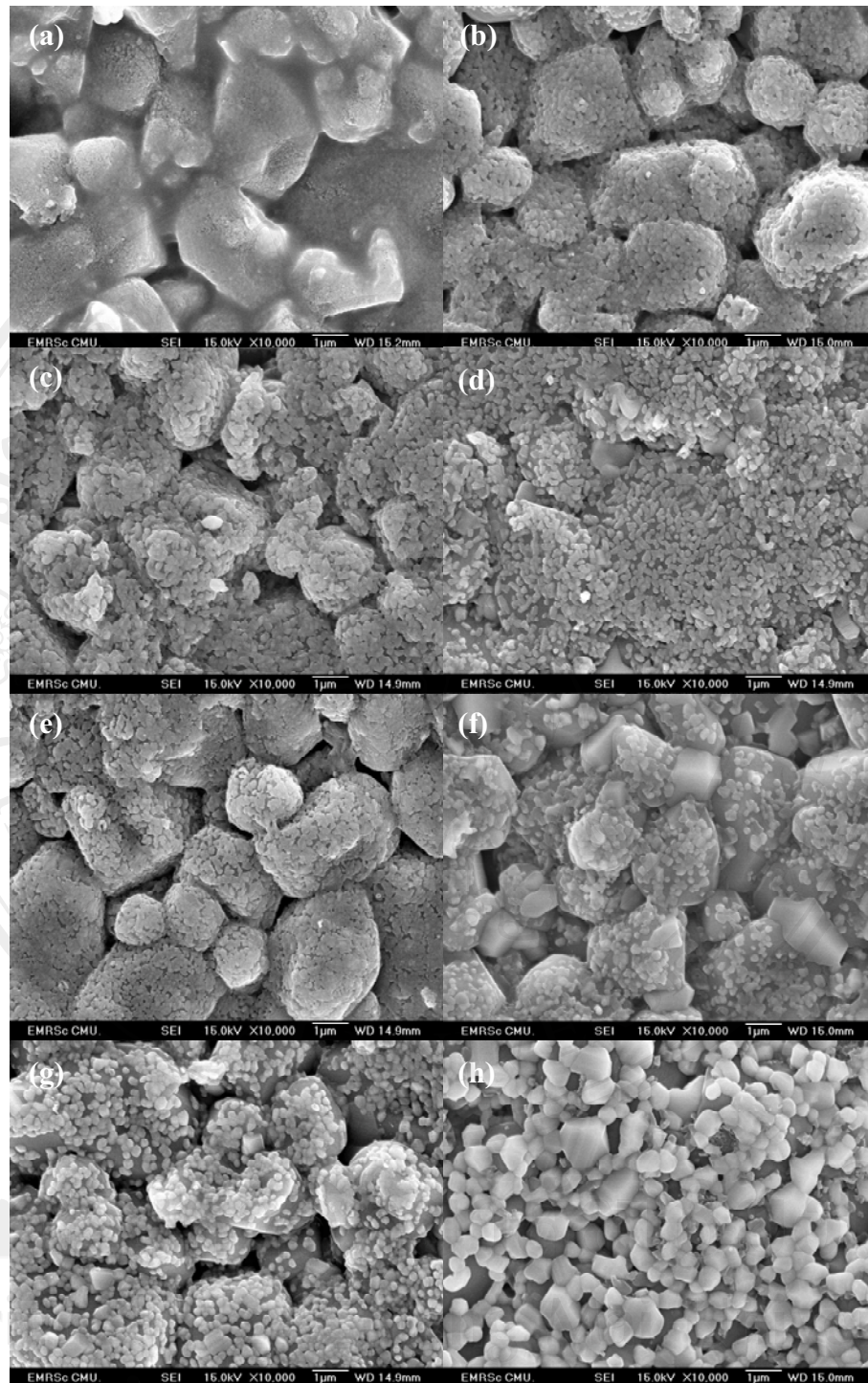


Figure 2.23 the FE-SEM top view images of copper thin films by thermal oxidation reaction for (a) not anneal (b) at 300°C for 48 hr, (c) at 400°C for 48 hr, (d) at 500°C for 48 hr, (e) at 600°C for 48 hr, (f) at 700°C for 48 hr, (g) at 800°C for 48 hr and (h) at 900°C for 12 hr.

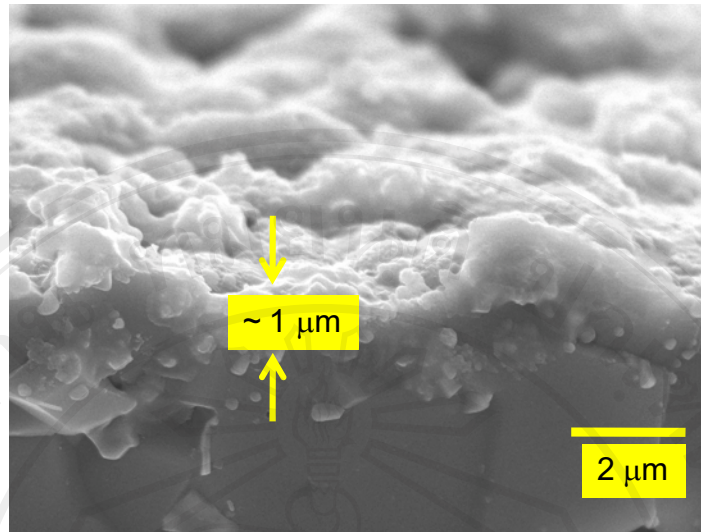


Figure 2.24 FE-SEM cross-sections of CuO thin films.

2.3.4.2 EDS result of CuO thin films by thermal evaporated copper thin films

The EDS spectrum of CuO thin films shown in figure 2.25 proves that the synthesized sample is composed of Al, Cu and O elements with atomic% of O=58.90, Al =25.56 and Cu=15.55 % as shown in table 2.5. However the result of the EDS spectrum cannot confirm that the structure of the evaporation sample is CuO and Al₂O₃.

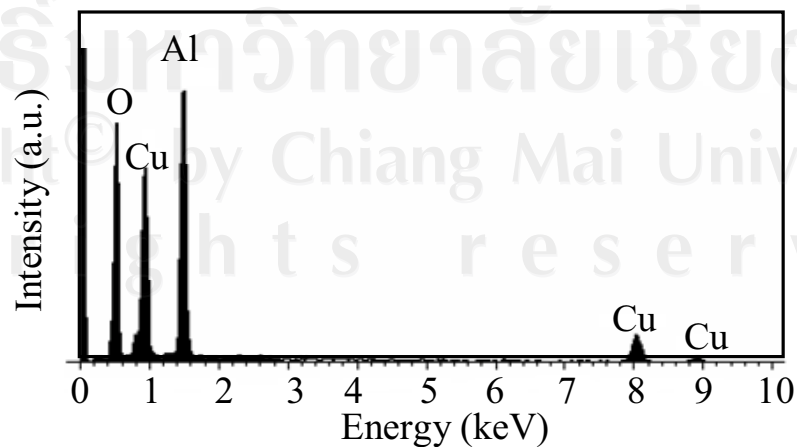


Figure 2.25 EDS spectrum of CuO thin films.

Table 2.5 Element content of CuO thin films on alumina substrate

Element	Weight%	Atomic%
O	35.97	58.90
Al	26.32	25.56
Cu	37.71	15.55
Totals	100.00	100.00

2.3.4.3 XRD result of CuO thin films by thermal evaporated copper thin films

XRD was used to confirm the chemical composition of the sample. Figure 2.26 shows the XRD spectrum of CuO thin films. The XRD results show that CuO is the main oxidation products with a small amount of Cu, Cu₂O and Al₂O₃ (alumina substrate) after oxidation at 800 and 900°C. This result suggests that the films are non-single phase within the instrumental detection limits of XRD analysis (Fig. 2.26). The diffraction peaks at $2\theta = 35.32^\circ$, 37.92° , 61.40° , 66.64° and 68.32° can be assigned to the (111), (111), ($\bar{1}13$), ($\bar{3}11$) and (220) planes of crystalline CuO, respectively. These peaks match with reported data for CuO (JCPDS 45-0937). The peaks at $2\theta = 29.36^\circ$ can be assigned to the (110) planes of crystalline Cu₂O. These peaks match with reported data for Cu₂O (JCPDS 03-0839). The peaks at $2\theta = 52.68^\circ$ and 57.64° can be assigned to the (024) and (116) planes of crystalline Al₂O₃. These peaks match with reported data for Al₂O₃ (JCPDS 47-1771). The peaks at $2\theta = 43.48^\circ$ can be assigned to the (110) planes of crystalline Cu. These peaks match with reported data for CuO (JCPDS 04-0836). It was found that, the oxidation reaction of copper thin films had two phases these confirm by equation (2.1) and (2.2) phases are Cu₂O and CuO structure, respectively.

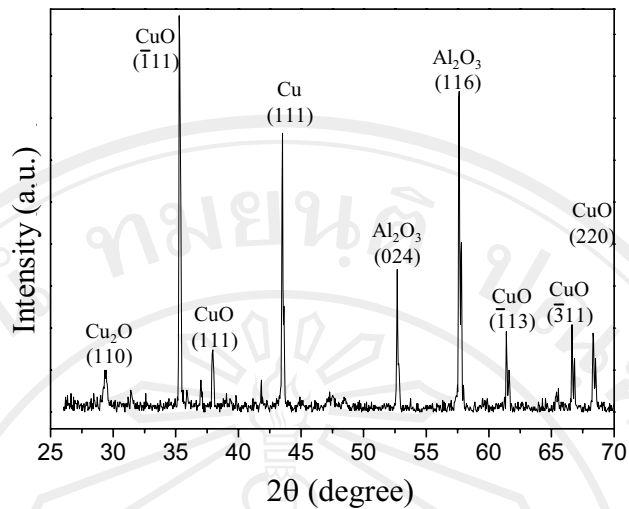


Figure 2.26 XRD spectrum of CuO thin films.

2.3.4.4 Raman spectra result of CuO thin films by thermal evaporation

Figure 2.27 presents the Raman spectra of nanocrystal CuO samples. It can be seen that there are three Raman peaks in sample A, at 282, 332, 618 cm^{-1} , with the second one being weakest and the third being broad. In comparison with the vibrational spectra of a CuO single crystal as shown in figure 2.19, we can assign the peak at 282 cm^{-1} to the Ag mode and the peaks at 332 and 618 cm^{-1} to the Bg modes.

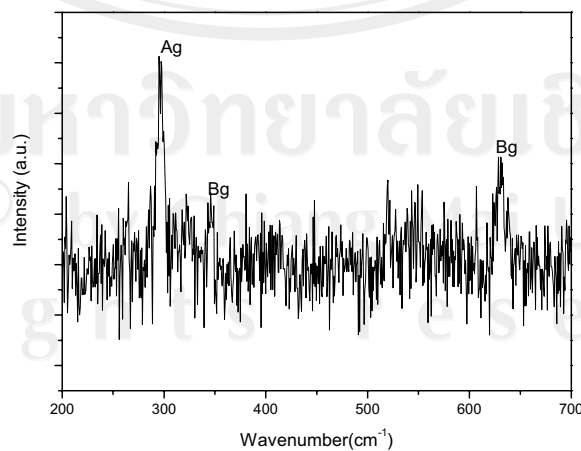


Figure 2.27 Raman peaks of annealed copper thin films on alumina.